Applied Nanoscience (2022) 12:225–236
https://doi.org/10.1007/s13204-021-02284-7

ORIGINAL ARTICLE

Safety studies of polyethylene glycol–hydroxyapatite nanocomposites on *Drosophila melanogaster*: an in vivo model

Pallavi Dan[1] · Swetha Senthilkumar[1] · Devanand Venkatsubbu Gopinath[2] · Sahabudeen Sheik Mohideen[1]

Received: 4 October 2021 / Accepted: 27 November 2021 / Published online: 14 January 2022

Abstract
Hydroxyapatite Nanoparticle (HAp NPs) is similar to the crystal structure of human bone. It has excellent properties such as biocompatibility, osteoconductivity, and biodegradable. Owing to these properties, it has been used in the field of drug delivery, dental applications, and bone tissue engineering. PEG (Polyethylene glycol) is a synthetic biodegradable polymer. It prevents the agglomeration of the nanoparticles, surface oxidation of the particles and thereby making it more biocompatible. Rose Bengal (RB) is a photo sensitiser which has the ability to generate singlet oxygen. In the present study, PEG/HAp nanocomposite has been synthesised and characterised using DLS and Zeta potential, TEM, and FTIR. The safety efficacy of the PEG/HAp nanocomposite was studied in wild type Drosophila larvae and adult flies after oral administration. Larval crawling assay, negative geotaxis assay, survival assay, biochemical assays—SOD activity, DPPH activity and GSH activity were performed. This study showed that the nanocomposite did not affect the development of the larva rather it enhanced the behavioural and antioxidant activity. In the adult flies, the climbing activity and the survivability patterns were greatly improved. Earlier studies with HAp NPs on the *Drosophila* model did not enhance behavioural and antioxidant activities whilst in the present study, PEG might help in improving these activities due to its non-immunogenic and non-antigenic properties.

Keywords HAp NPs · PEG · PEG/HAp nanocomposite · *Drosophila melanogaster*

Introduction

Calcium phosphate (CaP) is a generic name given to any compounds made up of calcium and phosphate ions as its core structure. The group of compounds belonging to the CaP family also sometimes include calcium ions linked with other functional groups such as ortho meta or pyrophosphates in addition to hydroxide or hydrogen ions. Some of the key players in the CaP family are hydroxyapatite (HAp), dicalcium phosphate (brushite) and calcium orthophosphates that are naturally abundant in the vertebrate skeletal systems (Nosrati et al. 2021; Zhu 2017). CaP family nanomaterials are known for their large surface area, biocompatibility, increased drug loading capacity, desirable drug release effects and bioactivity. These factors makes the CaP family nanocompounds to be effective drug delivery carriers, additionally, HAp conjugates were observed to serve as a scaffold thereby promoting bone defect restoration and high gene loading capabilities (Zhu 2017). In addition, Zinc–HAp nanorods showed great antibacterial properties whereas HAp sheets and HAp papers were shown to possess high adsorption capacity for heavy metal ions and organic pollutants, respectively (Lu et al. 2014; Zhu, 2017).

Hydroxyapatite (HAp) belonging to the apatite family of minerals specifically consists of Ca/P molar ratios within the range of 1.5–1.67 whilst also sharing a similar crystallographic structure with Fluorapatite and Oxyapatite (Canillas et al. 2017). HAp being extremely biocompatible and also known for its bioactive properties is highly preferred for medical applications (Teixeira et al. 2009; Kalita et al. 2007). Due to its stability and biocompatibility, HAp NPs are preferred to be used for implants, bone substitutes, and oral treatment (Mostafa and Brown 2007). Unique configuration and specific surface area of these NPs have created

✉ Sahabudeen Sheik Mohideen
sahabuds@srmist.edu.in

[1] Department of Biotechnology, School of Bioengineering, SRM Institute of Science and Technology, Kattankulathur, Tamil Nadu 603203, India

[2] Department of Nanotechnology, SRM Institute of Science and Technology, Kattankulathur, Tamil Nadu 603203, India

a new aspect for drug delivery applications in the field of medical sciences. The synthesis or the occurrence of the CaP family materials can be natural sources like that of HAp from bovine bones and eggshells (carboxy–HAp), or synthetic through high-temperature treatment or precipitation (Canillas et al. 2017).

The application HAp nanoparticles or nanocomposites are wide as discussed earlier, however, it was observed that the stability, mechanical and physical properties of HAp-based materials can be enhanced by slightly modifying the synthesis methods or by combining it with other composite materials, this was well studied in (Nosrati et al. 2020a, b, c). It was reported that modifying the synthesis method of HAp NPs by switching to argon-gas-injection solvothermal synthesis significantly increased the nanomaterial crystal and particle size along with the better crystallinity (Nosrati et al. 2020a, b, c). They have also specified the importance of altering the pressure and temperature significantly increased the parameters of the HAp nanorods thereby indicating preferential growth directions. Similar study reported in Nosrati et al. (2020a, b, c) showed that using hydrothermal autoclave with argon-15% hydrogen gas injection systems for synthesis, there was a significant improvement in the mechanical nature like crystallinity of reduced graphene oxide/hydroxyapatite (rGo/HA) composites. Another study by Nosrati et al. (2020a, b, c) demonstrated the fabrication of three-dimensional reduced graphene oxide/hydroxyapatite (HA)/Gelatin scaffolds by synthesising the nanopowder using a hydrothermal autoclave with hydrogen gas injection systems and the scaffold were prepared using hydrogel 3D-printing method. The modified fabrication process provided small pore size and increased dimensional accuracy in the scaffolds (Nosrati et al. 2020a, b, c).

Polyethylene glycol or PEG is a hydrophilic compound with its structure comprising of an inert polyether chemical backbone and terminal hydroxyl groups (HO-$(CH_2CH_2O)_n$-H). PEG plays a key role in the agglomeration of the nanoparticles and also effectively prevents the oxidation of the particle surface. In addition, PEG coating is also known to increase the circulation time and establish significant resistance to the plasma proteins (Photos et al. 2003). Owing to its benefits, application of PEG has been widely implemented across several industrial productions such as cosmetics, food additives, plasticisers, protein adsorption, cell adhesion, and drug delivery systems to name a few.

Conjugation of nanomaterials with PEG also known as pegylation and has several advantages. (Hu et al. 2018; Siepmann et al. 1999; Kim et al. 2005; Laskar et al. 2016; Niedermayer et al. 2015; Zeng et al. 2017). Studies have shown that PEG-based polymer micelles showed cytotoxic effects (Eckman et al. 2012), but zinc oxide functionalised PEG had shown decreased cytotoxicity in cancer cells. In addition, PEG can chelate Ca^{2+} of HAp NPs (Li et al. 1996) and its unique physiochemical properties have been utilised for applications like drug delivery (Huang et al. 2010). Nanocomposites using HAp NPs are embedded in the polymer matrix (Pramanik et al. 2006) of PEG, polyvinyl alcohol, polystyrene polymers to overcome the mechanical problems associated with bio ceramics for tissue engineering applications. PEG/HAp nanocomposite has been synthesised under a controlled environment for comparing their synergistic effects and to assess their biological potential to be used as smart materials for biomedical applications (Dhanalakshmi, 2012). Conjugating gold nanoparticles with PEG reduced the activation of platelets and also reduced cytotoxicity (Niidome et al. 2006). When silver nanoparticles were coated with PEG and lipoic acid, the cytotoxicity against human cells was reduced as compared to non-functionalised silver nanoparticles. The antibacterial and antibiofilm activity was improved (Milla and Cattel 2012; Niska et al. 2016; Ragaseema et al. 2012). Manna et al. showed that PEG functionalised with HAp NPs showed great biocompatibility with human fibroblasts cells. Structural, electrical, and in vitro kinetic studies were performed to study the effects of HAp/PEG composite for drug delivery application. It was observed that the drug release of aceclofenac drug was more when coated with HAp/PEG composite rather than HAp NPs alone (Manna et al. 2016). In addition, the nanocomposite was found to be extremely biocompatible with human dermis fibroblasts cells (Pramanik et al. 2015). PEG-coated HAp NPs loaded with silver nanoparticles had a synergistic antibacterial effect against *E. coli*. In the study by Bhowmick et al. showed that nanocomposites of chitosan, PEG and Hap–zinc oxide showed improved antibacterial activity and were found to be biodegradable. Moreover, the synthesised nanocomposite helped in the growth and proliferation of osteoblast like cells and had shown good cytocompatibility. Therefore, the synthesised nanocomposites have great potential for bone tissue engineering applications (Bhowmick et al. 2015).

Rose Bengal (RB) is a photosensitiser which has the ability to generate singlet oxygen. It is comprised of a xanthene ring. The C9 position of it is substituted by tetrachloro benzoic acid. It has been mainly used in eye drops for the identification of damaged conjunctival and corneal cells in the eyes. The pharmacokinetic properties of RB were studied in rats, rabbits, guinea pigs, and dogs. The study reported that RB had a half-life of 30 min in rats and rabbits, 46 min in dogs when administered with a dose of 0.01–10 mg/kg (Klaassen 1976). In another study, RB was found to be toxic at a concentration of 100 µM in breast cancer and melanoma cell lines. In case of breast cancer cells, the toxicity was observed at a concentration of 300 µM, whereas in melanoma cells, it was toxic at a concentration of 200 µM (Mousavi et al. 2006; Mousavi and Hersey 2007). Koevary studied the toxicity of RB on

ovarian carcinoma cells. When cells were cultured with RB for 4 days, at 50 µM concentration, the growth of the cells was supressed and maximum suppression occurred at 400 µM and 800 µM concentrations. Cell damage occurred due to RB-induced apoptosis and accumulation of ROS in the ovarian cancer cells (Koevary 2012). In the study by Mohideen et al (2015), the accumulation of tau was found to be reduced in human tau expressing flies, and improvement in the climbing activities of fly was observed when treated with RB. RB has been used for anti-cancer therapy, which can produce cytotoxic singlet oxygen when irradiated by light to kill the tumour cells. However, RB has a very faster rate of elimination and lower rate of tumour formation due to this, the in vivo applications of RB are limited (Oliveira et al. 2006) (Hiraoka et al. 2006). The study by Shrestha et al. (2012) showed that RB conjugated chitosan had lower cytotoxicity and also, the ability to cross-link and reinforce dentin collagen matrix to enhance resistance to degradation and improve its mechanical properties (Shrestha et al. 2012).

Drosophila melanogaster is a robust model organism used in research lab. Moreover, homologous genes and organs in both humans and flies make it easier for studying numerous diseases and their dynamic genetic, cellular, and physiological mechanisms (Pandey and Nichols, 2011). Flies have been used for studying the toxicity of various nanoparticles, their biocompatibility, and their mode of action (Ahamed et al. 2010; Alaraby et al. 2016; Jovanović et al. 2016; Pappus et al. 2017; Posgai et al. 2009). Only a few studies are available wherein flies have been used as a model for in vivo screening of carrier molecules and drug release studies (Ferguson et al. 2018; Su 2019).

In the present study, PEG/HAp nanocomposites were synthesised and the effects of this composite on the larva and adult flies have been studied. Locomotory assays such as crawling assay in larva and negative geotaxis assay in adult flies have been performed. Biochemical assays such as SOD activity, GSH, and DPPH activity were also performed. In addition, Rose Bengal (RB) has been used as a drug for studying the drug loading and release patterns.

Materials and methods

Agar–agar type I, sodium phosphate monobasic, and sodium phosphate dibasic were procured from HiMedia, Mumbai. D-glucose, potassium chloride, yeast extract powder, tetra sodium pyrophosphate decahydrate, NADH, phenazolium methosulfate (PMS), and sodium sulphate were purchased from SRL Chemicals, Mumbai. PEG 6000 and Rose Bengal disodium salt were procured from SRL Mumbai. All the reagents used were of analytical grade.

Synthesis of PEG–HAp nanocomposite

HAp NPs were mixed with 1% PEG 6000 solution and stirred overnight. The solution was centrifuged at 18,000 rpm, 10 min, 4 ℃. The pellet was rinsed with Milli Q water and dried at room temperature (Venkatasubbu et al. 2013).

Characterisation studies

TEM study: The morphology of the synthesised HAp/PEG nanocomposite was observed through a JEOL JEM-2100 transmission electron microscope (TEM). The sample was placed on a copper grid at room temperature without staining.

SEM analysis: The morphological features of the synthesised HAp/PEG nanocomposite were studied using Thermoscientific Apreo S scanning electron microscope (SEM). The sample was placed on an aluminium foil and then loaded onto carbon-coated grid at room temperature.

FTIR study: To analyse the possible chemical interactions between HAp and PEG, FTIR spectroscopy measurements were obtained with a Shimadzu taken in IRTracer-100-Shimadzu spectrometer operated in the transmission mode in the range from 4000 to 400 cm^{-1}. The powdered sample was mixed with KBr powder and pressed into discs for the measurements.

XRD study: XRD patterns HAp/PEG nanocomposite were obtained with a in a Bruker US D8 Advance. The XRD patterns were collected at room temperature in the 2θ, scanning range from − 10° to − 80°.

Dynamic light scattering (DLS) and Zeta Potential: The size distribution and charge of the HAp/PEG nanocomposite was analysed using Dynamic Light Scattering Spectrometer-Particle Size analyser and Zeta Potential, Horiba-SZ-100-Z, Japan. The concentration of the samples used for analysis was 0.01 wt % in deionised water. 0.01 M sodium chloride solution was used to analyse the zeta potential of the samples.

Drosophila husbandry

Oregon K, wild-type flies were used in the present study. Flies were grown in standard cornmeal agar at 25 ± 1 ℃, 60% relative humidity, and 12 h light and dark cycle.

Experimental setup

The experimental setup had the following doses: control, 10 µg/ml, 100 µg/ml, and 1000 µg/ml, respectively. In each vial, 15 adult male and female flies were added. After 48 h, the parents were discarded. The larvae were used for

crawling assay and biochemical assays. The new born adult flies were exposed to the treatment food for 15 days.

Crawling assay

To study the locomotory behaviour of the larva, the protocol of Sundararajan et al. was followed (Sundararajan et al. 2019). Briefly, third instar larvae were collected and rinsed with water, to remove any food traces. The larvae were made to crawl on a smooth agar surface. A graph sheet was placed beneath the plate. A 1-min video was recorded and the distance covered by the larva was calculated ($n = 9$).

Negative geotaxis assay

A previously optimised protocol was followed to study the climbing ability of the flies (Sundararajan et al. 2019). Twenty-five adult male flies were added to the respective treatment vials and control vials and maintained for 15 days. After the treatment period was over, the flies were transferred to an empty vial having 3 cm mark on it. The vials were tapped for few seconds so as all the flies remained at the bottom. A video was recorded for 1 min and the number of flies above the 3 cm mark was counted.

Survival assay

The survival assay was executed according to the protocol by Mohideen et al. (2015). 100 adult male flies were transferred to the respective treatment and control vials. The vials were monitored every day to count the no of dead flies. Those flies which escaped or stuck to the food were excluded. Once all the flies were dead, a survival curve was plotted. Log-rank Mantel–Cox test was performed using Graph pad prism 6 software, to analyse the statistical difference between the treatment and control groups.

Superoxide dismutase activity

SOD activity in larva and flies was determined according to the protocol of Ahmed et al. (2010). 20 third instar larva/male flies were homogenised in 0.5 ml of 0.1 M phosphate buffer (pH 7.4) and centrifuged at 6000 rpm, 10 min at 4 ℃. To initiate the reaction, 0.2 ml of 780 µM NADH was added to the mixture comprising of 1 ml of 0.052 M sodium pyrophosphate buffer (pH 8), 0.1 ml of 186 µM phenazine methosulphate, 0.3 ml of nitroblue tetrazolium, 0.2 ml supernatant and 0.2 ml of Milli Q water. The reaction was stopped after 1 min by adding 1 ml of glacial acetic acid. The OD was measured at 560 nm. One unit of enzyme activity is defined as the enzyme activity required to inhibit 50% of chromogen production at room temperature.

DPPH activity

The protocol of Bag and Mishra was followed with few modifications. In 0.1 mM of sodium phosphate buffer, 25 larvae/ flies were homogenised followed by centrifugation at 10,000 rpm, 10 min 4 ℃. 2.5, 5, 10, and 20 µl of the sample were taken. To this, 125 µl of DPPH and 50 µl of absolute methanol were added and incubated for 30 min. OD was measured at 517 nm (Bag and Mishra 2020).

GSH activity

GSH activity was performed according to the protocol of Ellman 1959 (Ellman 1959). Briefly, 0.1 ml of the homogenate and 0.9 ml of 5% TCA were centrifuged at 2300*g* for 15 min at 4 ℃. Then, 0.5 ml of supernatant was added to 1.5 ml of 0.1% DTBN and the OD was read at 412 nm. The amount of GSH was expressed in nmol/mg of protein.

In vitro drug loading studies and release studies of Rose Bengal

Drug loading

Rose Bengal (RB) was loaded onto HAp/CS nanocomposite according to the protocol by Venkatasubbu et al. (2011). 100 mg of PEG/HAp nanocomposite was added to the Rose Bengal solution and stirred for 20 min. The suspension was centrifuged at 5000 rpm for 10 min. The absorbance of the supernatant was measured at 550 nm. The amount of drug loaded is determined by the difference in the concentration of RB before and after adsorption. The drug loading percentage was calculated using the following formula:

$$[(X - Y)/X \times 100],$$

where X and Y are the initial and final concentrations of RB solution.

Drug release profile

The drug release profile of RB loaded onto HAp/PEG nanocomposite was studied. 100 mg of drug-loaded nanocomposite was added to phosphate buffer saline (PBS, pH 7.4). At different time intervals, 2 ml of sample was withdrawn and replaced with 2 ml of PBS. The OD was measured at 550 nm.

Statistical analysis

The values are expressed as mean ± SEM. GraphPad Prism 6.0 software was used to check the statistical significance between control and treated groups, respectively.

Results

Characterisation of PEG/HAp nanocomposite

The size and charge of the nanocomposite were analysed using DLS and Zeta potential. The size of the nanocomposite was found to be 5162.9 nm and the zeta potential was − 25 mV, respectively. The morphological features of the synthesised nanocomposite were studied using SEM and TEM analysis. The SEM image of the nanocomposite is shown in Fig. 1a. The nanocomposite was found to be aggregated thus showing that the polymer is embedded over the matrix of the HAp NPs. TEM image of the HAp/PEG nanocomposite is shown in Fig. 1b. The synthesised nanocomposite was rod shaped with an average size of 50 nm. The HAp NPs are embedded in the matrix of the polymer. The FTIR spectrum of HAp/PEG nanocomposite is shown in Fig. 2. The absorption peak at 1110 cm^{-1} corresponds to C–O–C stretching and vibration of the repeated $–OCH_2CH_2–$ units of the PEG backbone. In PEG/HAp nanocomposite, this peak is shifted to 1105 cm^{-1}, wherein a hydrogen bond is formed between PEG and HAp NPs. In the area with 3335 cm^{-1}, the OH stretching vibration is observed in PEG and it is shifted to 3428 cm^{-1} in PEG/HAp nanocomposite, thus exhibiting a hydrogen bond. The presence of distinctive absorption peaks of PEG such as C–O–C antisymmetric stretching, 1342 cm^{-1}) and –CH at, 955 cm^{-1} peaks in the FTIR spectrum of PEG and PEG/HAp nanocomposite suggested that PEG was grafted to the HAp Nps (Venkatasubbu et al. 2013). The crystalline phase structures of HAp and HAp/PEG nanocomposite were analysed using XRD. The XRD patterns of HAp and HAp/PEG are shown in Fig. 3a and b. The peaks observed at $2\theta = 26.4°$, 32.1°, 40.6°, and 43.7° are attributed to (211), (112), (013), and (113) crystalline planes of HAp NPs with d spacing 5.27 Å, (JCPDS card no 98-006-8674). The diffraction of the peaks can be observed in the HAp/PEG nanocomposite. The intensity of (112) plane is decreased in the HAp/PEG nanocomposite. This shows that PEG is coated over the HAp NPs.

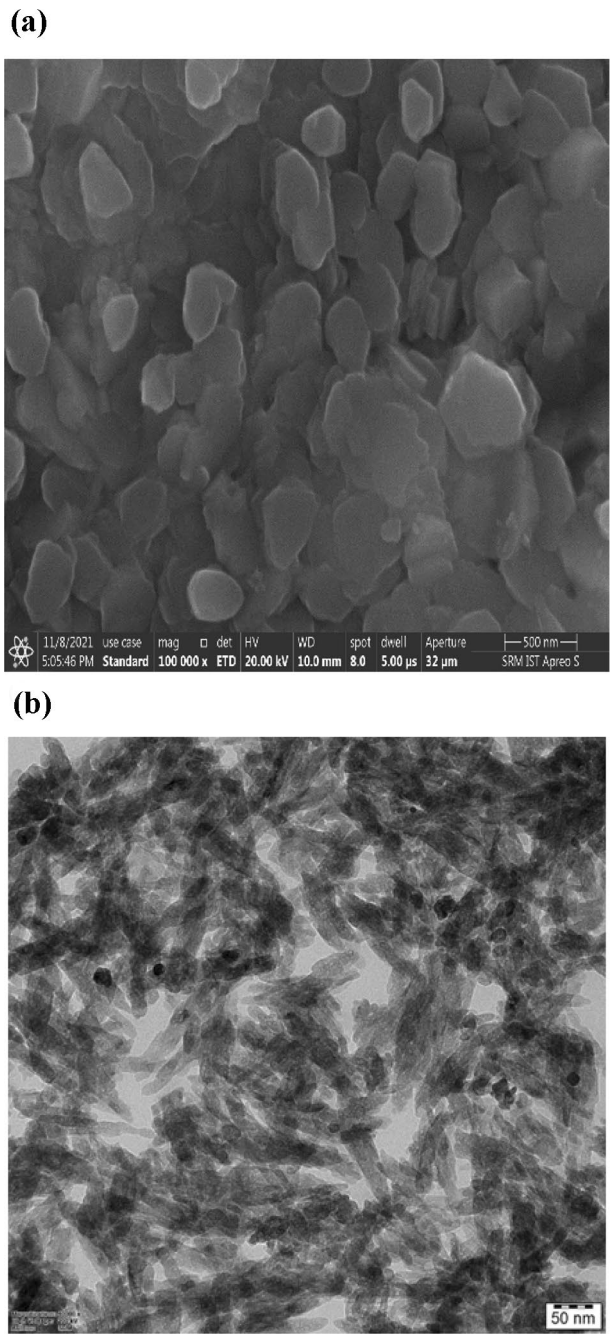

Fig. 1 **a** SEM image of PEG/HAp nanocomposite. **b** TEM image of PEG/HAp nanocomposite

Crawling assay

The larval crawling activity is shown in Fig. 4. Crawling activity is performed to check if any degeneration occurs in their locomotory activity due to the toxic nature of nanoparticles. The average distance crawled by the larvae in control was 26.5 mm and 43.1 mm in 10 µg/ml, 30.18 in 100 µg/ml, and 48.14 mm in 1000 µg/ml, respectively. A significant increase in crawling activity was observed in 10 µg/ml and 1000 µg/ml with respect to control.

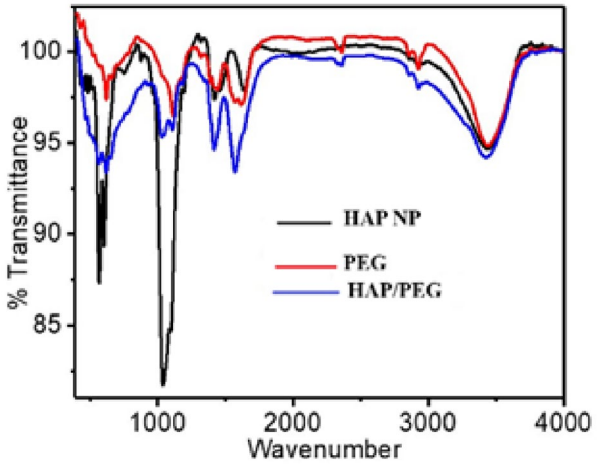

Fig. 2 FTIR spectra of PEG/HAp nanocomposite

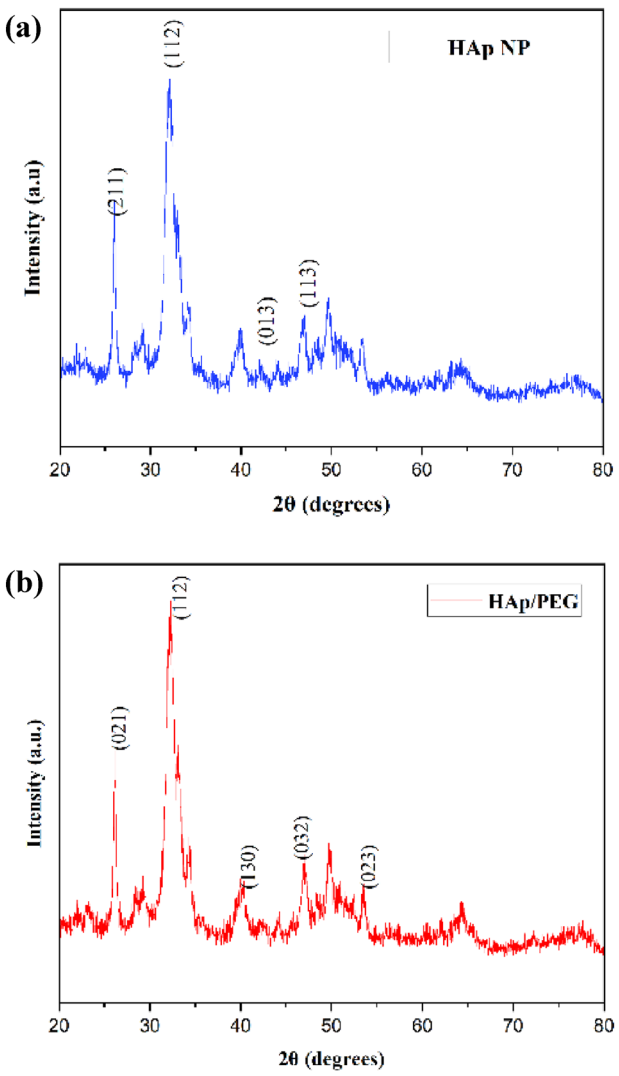

Fig. 3 XRD patterns of **a** HAp NPs and **b** HAp/PEG nanocomposite

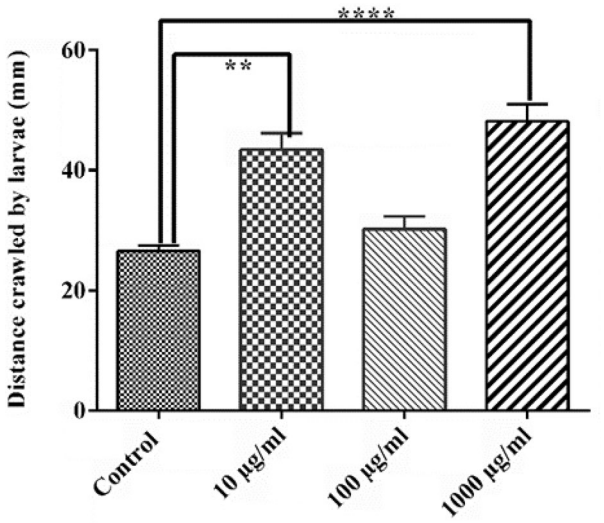

Fig. 4 Crawling activity of larvae treated with PEG/HAp nanocomposite. Values are represented as mean ± SEM

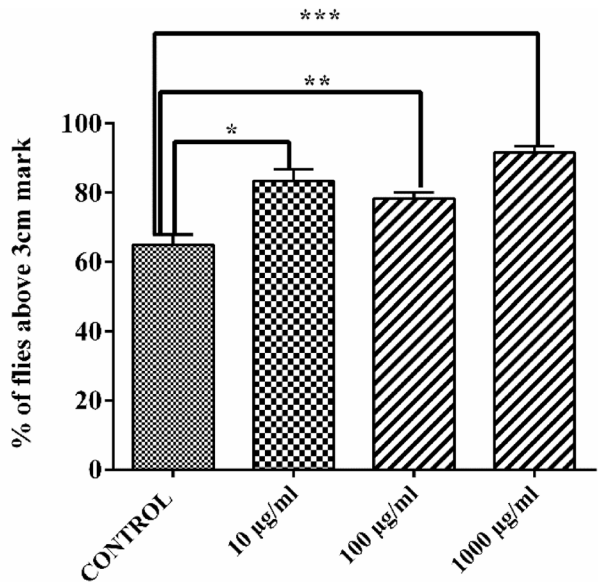

Fig. 5 Negative geotaxis assay of adult flies treated with PEG/HAp nanocomposite. Values are represented as mean ± SEM

Negative geotaxis assay

Negative geotaxis assay is used for assessing neurodegeneration and also to evaluate the effect of nanoparticles on the climbing activity of the flies. In the present study, a significant increase in the climbing activity of the flies in the treatment groups with respect to control, respectively, is shown in Fig. 5.

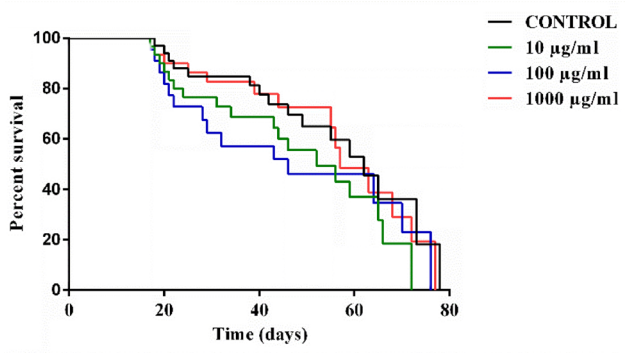

Fig. 6 Survival assay of adult male flies

Survival assay

The survivability curve is shown in Fig. 6. The survival assay was performed to evaluate if there was any kind of toxicity induced by the PEG–HAp nanocomposite. The flies survived for 70 days in both the treatment and control vials. No statistical significance was observed amongst the curves of the log-rank Mantel–Cox test.

Superoxide dismutase activity

Figure 7 shows the SOD activity of the larvae and adult flies treated with the nanocomposite. To evaluate the toxicity of nanoparticles, SOD activity is measured. Significant increase in the levels of SOD activity leads to toxicity of nanoparticles. In the present study, there was a significant decrease in the activity in 10 µg/ml and 100 µg/ml with respect to control was observed in larvae. No significant changes were observed in the activity of adult male flies.

DPPH activity

The DPPH activity is performed to study the level of antioxidants. In the present study, the DPPH activity significantly increased in the larva and adult flies when compared with the control (Fig. 8).

GSH activity

GSH is a predominant antioxidant found in the brain. Its function is to react with ROS and other nucleophilic compounds to combat oxidative stress under normal conditions. A significant decrease in the GSH activity was observed in larvae and adult flies, when exposed to PEG, coated HAp nanocomposite (Fig. 9).

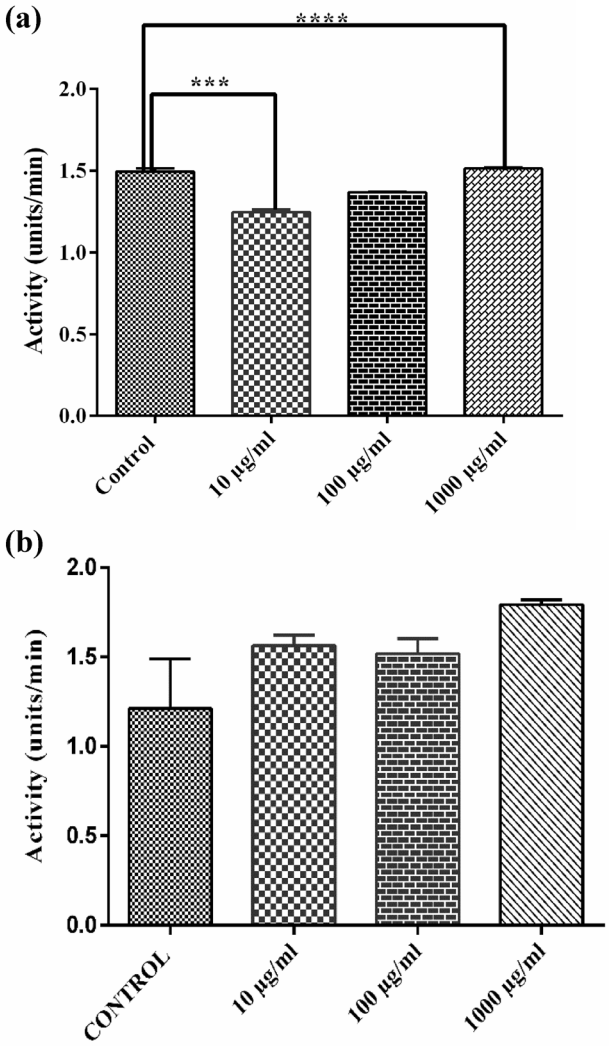

Fig. 7 **a** SOD activity of larvae treated with PEG/HAp nanocomposite. **b** SOD activity of adult male flies treated with PEG/HAp nanocomposite. Values are represented as mean ± SEM

In vitro drug loading and release studies of Rose Bengal

RB was loaded onto HAp NPs before coating with PEG to decrease the initial burst thereby slowing down the drug release. The percentage of RB-loaded HAp NPs was found to be 17.3% whereas the drug loading percentage of RB loaded on PEG/HAp nanocomposite was 83.1%.

To check if PEG-coated HAp NPs prolonged the release of RB, RB-loaded PEG/HAp nanocomposite was dispersed in PBS solution. The drug release for RB without PEG coating was found to be 32.5% after 29 h, whereas the drug release with the PEG coating was found to be 95.16% after 33 h, respectively. As a result, a faster release of RB occurs from the HAp/PEG nanocomposite when compared to the HAp NPs (Fig. 10).

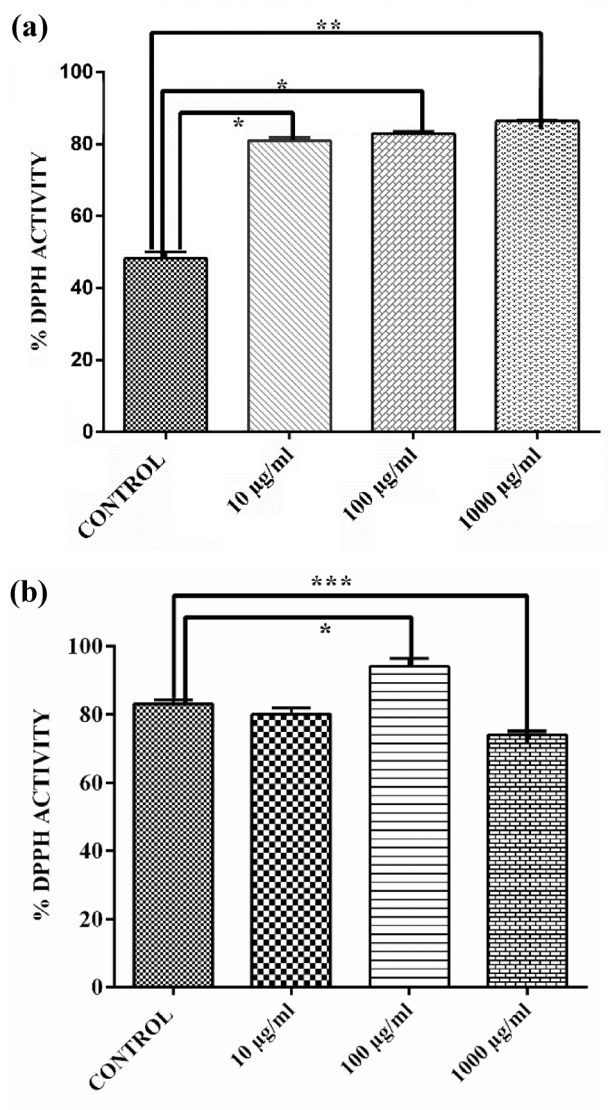

Fig. 8 **a** DPPH activity of larva treated with PEG/HAp nanocomposite. **b** DPPH activity of adult male flies treated with HAp/PEG nanocomposite. Values are represented as mean ± SEM

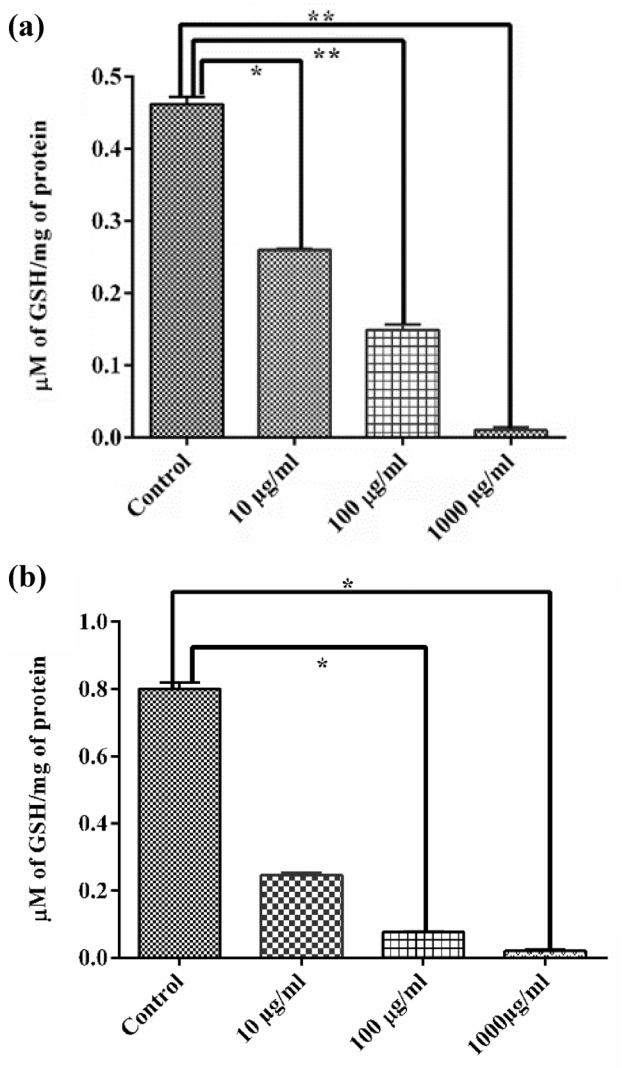

Fig. 9 **a** GSH activity of larva. **b** GSH activity of adult male flies treated with PEG/HAp nanocomposite. Values are represented as mean ± SEM

Discussion

HAp NPs based bio-analogue composites have been designed using different polymer matrices such as polymethyl methacrylate, high-density polyethylene, and poly L-lactide for bone tissue engineering applications. The proportion of surface area to volume is higher in HAp NPs; a small amount of the material is adequate to increase its bioactivity. The interfacial bond between the matrix helps in e improving the mechanical strength of the HAp NPs/polymer composites (Pramanik et al. 2006). PEG has various beneficial properties such as a varied range of molecular weights, highly water-soluble, lower toxicity, and flexible chains. It can also be extracted from different forms of non-toxic metabolites. Polymeric materials are often being used for stabilising metal colloids, thereby the agglomeration and precipitation of the materials are prevented (Chen and Huang 2002). PEG can form complexes with metal cations due to the presence of ether oxygen groups in its chain. The physical properties of the metals such as thermal stability and aggregation change when an interaction between PEG and metal cations occurs (Okada 1993). It has also been used to improve the efficacy of drug delivery to the targeted cells. In addition, the coating of PEG on the surface of the nanoparticle prevents the aggregation of the surface and the time of systemic circulation is prolonged. Attachment of PEG with the nanoparticles can be either covalent or noncovalent. A matrix is created by this attachment around the nanoparticles, which acts as a drug carrier (León et al.

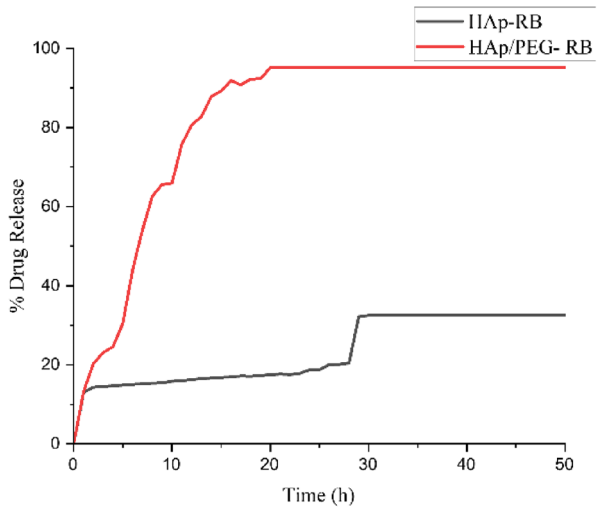

Fig. 10 Drug release study of RB loaded onto PEG/HAp nanocomposite

2017.). The study by Sapre et al. (2020) demonstrated the rhodamine release from mesoporous silica nanoparticles coated with PEG and PDA polymers in the gut of *D. melanogaster*. It was observed that PEG-coated particles showed better release of the drug when compared with PDA-coated particles (Sapre et al. 2020). In the study by Sundararajan et al. (2019), the potential of cerium oxide nanoparticles has been explored in both wild type and transgenic AD model flies. It was observed that both larvae and wild-type flies when exposed to 0.1 mM and 1 mM concentrations did not show any toxic effects as evident from the behavioural and biochemical assays (Sundararajan et al. 2019). In GMR h tau flies, the autophagy pathway was activated and the level of htau was also reduced. Whereas in elav; htau AD model, the levels of SOD enzymes were restored (Sundararajan et al. 2019, 2021). Furthermore, in another study by Sarkar et al. (2021), the therapeutic potential of cerium oxide nanoparticles against BPA toxicity in flies was tested. It was found that cerium oxide nanoparticles were able to lower the oxidative stress, genotoxicity and improved behavioural activity (Sarkar et al. 2021). In a previous study conducted by Dan et al. (2019), HAp NPs were found to be non-toxic at both lower concentration 10 µg/ml as well at 1000 µg/ml in both larvae and adult flies (Dan et al. 2019).

The movement in Drosophila larva occurs mainly due to the shrinkage of the body wall muscles and these muscles are regulated by the motor neurons in the ventral ganglion's dorsal region (Glanzman 2010). The crawling ability of the larvae is affected when exposed to any toxic compound or drug. In the present study, PEG/HAp nanocomposite significantly improved the crawling activity of the larvae. The negative geotaxis assay helps to evaluate the neurodegeneration and climbing defects in flies (Feany and Bender 2000; Linderman et al. 2012). Dietary exposure of PEG–HAp nanocomposite for 15 days showed a significant improvement in the climbing activity of the flies. Increased production of ROS leads to oxidative stress and toxicity in nanoparticles (Pappus et al. 2017). This in turn is reversed with the help of antioxidant enzymes (Nel et al. 2006) such as SOD, GSH, and DPPH. SOD is a free radical scavenging enzyme. There are three types of SOD present in the mammalian system. It converts the superoxide which is produced due to xenobiotics into oxygen and water. GSH is a tripeptide, acts as a scavenger in the reduced form of the free radicals produced due to lipid peroxidation. In the present study, the levels of SOD were not affected significantly in both larvae and adult flies. Although DPPH activity was found to significantly increase in the flies and larvae, a reduction in the levels of the GSH enzyme was observed.

Various factors such as properties of drug and polymer, ratio and drug–polymer interaction, method of particle preparation, and incorporating the drug influence the incorporation of the drug into the nanoparticles. Studies have shown that drugs can be either incorporated during the particle preparation or absorbed or adsorbed onto the surface of preformed particles. In the present study, Rose Bengal (RB) was loaded onto PEG/HAp nanocomposite. The drug loading and release profile for RB was studied. RB is a hydrophilic drug, having high protein binding. Due to its high extinction coefficient at 549 nm, it has been majorly used as a diagnostic agent. In the present study, RB was loaded onto PEG–HAp nanocomposite. It was observed that the loading efficiency of RB increased from 17.3 to 83.1%. Coating with PEG reduces the opsonisation of the protein. In addition, it helps the nanoparticles in escaping the reticuloendothelial system and thereby reducing the clearance rate. The drug release profile showed 95.16% release in 20 h. A gradual release of the drug occurs. Initially, a rapid outburst of the drug occurs. It is due to the molecules present closer to the surface. After this, a steady release of the drug occurs wherein the molecules bound to the surface of the polymer are released. After this, the drug diffuses through the pores that are present in the matrix of the polymer. Erosion of the polymer, hydrodynamic interaction, and columbic interaction, drug solubility, and interaction between the drug and polymer are important factors to be considered when the drug is released through the biodegradable polymer surface (Tzafriri 2000; Siepmann et al. 1999, 2006).

Conclusion

In the present study, PEG/HAp nanocomposite has been studied for the first time in the *D. melanogaster* model. The synthesised nanocomposite showed improved crawling activity in the larvae and climbing activity of the flies. An

enhancement in the levels of the biochemical enzymes in both larvae and flies can be observed. In addition, in in vitro drug release studies of RB, PEG-coated HAp NPs had a faster release of RB when compared to HAp NPs.

Acknowledgements The authors thank the department of biotechnology, SRM IST for the support. The authors acknowledge the HRTEM FACILITY at SRMIST setup with support from MNRE (Project No.31/03/2014-15/PVSE-R&D), Government of India.

Declarations

Conflict of interest The authors declare no conflict of interest.

References

Ahamed M, Posgai R, Gorey TJ, Nielsen M, Hussain SM, Rowe JJ (2010) Silver nanoparticles induced heat shock protein 70, oxidative stress and apoptosis in *Drosophila melanogaster*. Toxicol Appl Pharmacol 242(3):263–269. https://doi.org/10.1016/j.taap.2009.10.016

Alaraby M, Annangi B, Marcos R, Hernández A (2016) Drosophila melanogaster as a suitable in vivo model to determine potential side effects of nanomaterials: a review. J Toxicol Environ Health Part B 19(2):65–104. https://doi.org/10.1080/10937404.2016.1166466

Bag J, Mishra M (2020) Biochemical assays to detect the antioxidant level in *Drosophila melanogaster*. In: Mishra M (ed) Fundamental approaches to screen abnormalities in *Drosophila*. Springer Protocols Handbooks. Springer, New York. https://doi.org/10.1007/978-1-4939-9756-5_13

Bhowmick A, Pramanik N, Manna PJ, Mitra T, Raja Selvaraj TK, Gnanamani A, Das M, Kundu PP (2015) Development of porous and antimicrobial CTS–PEG–HAP–ZnO nano-composites for bone tissue engineering. RSC Adv 5(120):99385–99393. https://doi.org/10.1039/c5ra16755h

Canillas M, Pena P, De Aza AH, Rodríguez MA (2017) Calcium phosphates for biomedical applications. Bol Soc Esp Ceram Vidrio 56(3):91–112. https://doi.org/10.1016/j.bsecv.2017.05.001

Chen DH, Huang YW (2002) Spontaneous formation of Ag nanoparticles in dimethylacetamide solution of poly(ethylene glycol). J Colloid Interface Sci 255(2):299–302. https://doi.org/10.1006/JCIS.2002.8674

Dan P, Sundararajan V, Ganeshkumar H, Gnanabarathi B, Subramanian AK, Venkatasubu GD, Ichihara S, Ichihara G, Sheik Mohideen S (2019) Evaluation of hydroxyapatite nanoparticles-induced in vivo toxicity in *Drosophila melanogaster*. Appl Surf Sci 484:568–577. https://doi.org/10.1016/j.apsusc.2019.04.120

Devanand Venkatasubbu G, Ramasamy S, Ramakrishnan V, Kumar J (2011) Hydroxyapatite-alginate nanocomposite as drug delivery matrix for sustained release of ciprofloxacin. J Biomed Nanotechnol 7(6):759–767. https://doi.org/10.1166/jbn.2011.1350

Dhanalakshmi CP (2012) Synthesis and preliminary characterization of polyethylene glycol (PEG)/hydroxyapatite (HAp) nanocomposite for biomedical applications. Int J Phys Sci. https://doi.org/10.5897/IJPS11.1495

Eckman AM, Tsakalozou E, Kang NY, Ponta A, Bae Y (2012) Drug release patterns and cytotoxicity of PEG-poly(aspartate) block copolymer micelles in cancer cells. Pharm Res 29(7):1755–1767. https://doi.org/10.1007/S11095-012-0697-5

Ellman GL (1959) Tissue sulfydryl groups. Arch Biochem Biophys 82(1):70–77. https://doi.org/10.1016/0003-9861(59)90090-6

Feany MB, Bender WW (2000) A *Drosophila* model of Parkinson's disease. Nature 404(6776):394–398. https://doi.org/10.1038/35006074

Ferguson CTJ, Al-Khalaf AA, Isaac RE, Cayre OJ (2018) pH-responsive polymer microcapsules for targeted delivery of biomaterials to the midgut of *Drosophila suzukii*. PLoS ONE 13(8):e0201294. https://doi.org/10.1371/journal.pone.0201294

Glanzman DL (2010) Common mechanisms of synaptic plasticity in vertebrates and invertebrates. Curr Biol 20(1):R31–R36. https://doi.org/10.1016/j.cub.2009.10.023

Hiraoka W, Honda H, Feril LB, Kudo N, Kondo T (2006) Comparison between sonodynamic effect and photodynamic effect with photosensitizers on free radical formation and cell killing. Ultrason Sonochem 13(6):535–542. https://doi.org/10.1016/j.ultsonch.2005.10.001

Hu Y, Zhao Z, Harmon T, Pentel PR, Ehrich M, Zhang C (2018) Paradox of PEGylation in fabricating hybrid nanoparticle-based nicotine vaccines. Biomaterials 182:72–81. https://doi.org/10.1016/j.biomaterials.2018.08.015

Huang FW, Wang HY, Li C, Wang HF, Sun YX, Feng J, Zhang XZ, Zhuo RX (2010) PEGylated PEI-based biodegradable polymers as non-viral gene vectors. Acta Biomater 6(11):4285–4295. https://doi.org/10.1016/J.ACTBIO.2010.06.016

Jovanović B, Cvetković VJ, Mitrović TL (2016) Effects of human food grade titanium dioxide nanoparticle dietary exposure on *Drosophila melanogaster* survival, fecundity, pupation and expression of antioxidant genes. Chemosphere 144:43–49. https://doi.org/10.1016/j.chemosphere.2015.08.054

Kalita SJ, Bhardwaj A, Bhatt HA (2007) Nanocrystalline calcium phosphate ceramics in biomedical engineering. Mater Sci Eng C 27 441–449. https://doi.org/10.1016/j.msec.2006.05.018

Kim P, Kim DH, Kim B, Choi SK, Lee SH, Khademhosseini A, Langer R, Suh KY (2005) Fabrication of nanostructures of polyethylene glycol for applications to protein adsorption and cell adhesion. Nanotechnology 16(10):2420. https://doi.org/10.1088/0957-4484/16/10/072

Klaassen CD (1976) Pharmacokinetics of rose Bengal in the rat, rabbit, dog, and guinea pig. Toxicol Appl Pharmacol 38(1):85–100. https://doi.org/10.1016/0041-008X(76)90163-0

Koevary SB (2012) Selective toxicity of rose bengal to ovarian cancer cells in vitro. Int J Physiol Pathophysiol Pharmacol 4(2):99

Laskar P, Dey J, Ghoshkumar S (2016) Evaluation of zwitterionic polymersomes spontaneously formed by pH-sensitive and biocompatible PEG based random copolymers as drug delivery systems. Colloids Surf B 139:107–116. https://doi.org/10.1016/J.COLSURFB.2015.11.042

León A, Reuquen P, Garín C, Segura R, Vargas P, Zapata P, Orihuela PA (2017) FTIR and Raman characterization of TiO_2 nanoparticles coated with polyethylene glycol as carrier for 2-methoxyestradiol. Appl Sci. https://doi.org/10.3390/app7010049

Li S, Liu Q, De Wijn J, De Groot K, Zhou B (1996) Biomimetic coating of bioactives ceramic on bamboo for biomedical applications. J Mater Sci Lett 15(21):1882–1885. https://doi.org/10.1007/BF00264085

Linderman JA, Chambers MC, Gupta AS, Schneider DS (2012) Infection-related declines in chill coma recovery and negative geotaxis in *Drosophila melanogaster*. PLoS ONE 7(9):e41907. https://doi.org/10.1371/JOURNAL.PONE.0041907

Lu B-Q, Zhu Y-J, Chen F (2014) Highly flexible and nonflammable inorganic hydroxyapatite paper. Chemistry 20(5):1242–1246. https://doi.org/10.1002/CHEM.201304439

Manna A, Pramanik S, Tripathy A, Moradi A, Radzi Z, Pingguan-Murphy B, Hasnan N, Abu Osman NA (2016) Development of biocompatible hydroxyapatite-poly(ethylene glycol) core-shell nanoparticles as an improved drug carrier: structural and electrical

characterizations. RSC Adv 6(105):102853–102868. https://doi.org/10.1039/c6ra21210g
Milla P, Cattel FD (2012) Pegylation of proteins and liposomes: a powerful and flexible strategy to improve the drug delivery. Curr Drug Metab 13(1):105–119. https://doi.org/10.2174/138920012792783569
Mohideen SS, Yamasaki Y, Omata Y, Tsuda L, Yoshiike Y (2015) Nontoxic singlet oxygen generator as a therapeutic candidate for treating tauopathies. Sci Rep 5:1–14. https://doi.org/10.1038/srep10821
Mostafa NY, Brown PW (2007) Computer simulation of stoichiometric hydroxyapatite: structure and substitutions. J Phys Chem Solids 68(3):431–437
Mousavi S, Hersey P (2007) Role of caspases and reactive oxygen species in Rose Bengal-induced toxicity in melanoma cells. Iran J Basic Med Sci 2(34):118–123
Mousavi S, Dong Zhang X, Sharifi A, Hersey P (2006) Study of rose bengal-induced cell death in melanoma cells in the absence of light. Iran J Basic Med Sci 3(31):216–222
Nel A, Xia T, Mädler L, Li N (2006) Toxic potential of materials at the nanolevel. Science 311(5761):622–627. https://doi.org/10.1126/SCIENCE.1114397
Niedermayer S, Weiss V, Herrmann A, Schmidt A, Datz S, Müller K, Wagner E, Bein T, Bräuchle C (2015) Multifunctional polymer-capped mesoporous silica nanoparticles for pH-responsive targeted drug delivery. Nanoscale 7:7953. https://doi.org/10.1039/c4nr07245f
Niidome T, Yamagata M, Okamoto Y, Akiyama Y, Takahashi H, Kawano T, Katayama Y, Niidome Y (2006) PEG-modified gold nanorods with a stealth character for in vivo applications. J Control Release 114(3):343–347. https://doi.org/10.1016/j.jconrel.2006.06.017
Niska K, Knap N, Kędzia A, Jaskiewicz M, Kamysz W, Inkielewicz-Stepniak I (2016) Capping agent-dependent toxicity and antimicrobial activity of silver nanoparticles: an in vitro study. Concerns about potential application in dental practice. Int J Med Sci 13(10):772–782. https://doi.org/10.7150/ijms.16011
Nosrati H, Sarraf-Mamoory R, Le DQS, Perez MC, Bünger CE (2020a) Evaluation of argon-gas-injected solvothermal synthesis of hydroxyapatite crystals followed by high-frequency induction heat sintering. Cryst Growth Des 20(5):3182–3189. https://doi.org/10.1021/acs.cgd.0c00048
Nosrati H, Sarraf-Mamoory R, Le DQS, Zolfaghari Emameh R, Canillas Perez M, Bünger CE (2020b) Improving the mechanical behavior of reduced graphene oxide/hydroxyapatite nanocomposites using gas injection into powders synthesis autoclave. Sci Rep 10(1):1–13. https://doi.org/10.1038/s41598-020-64928-y
Nosrati H, Sarraf Mamoory R, Le Svend DQ, Bünger CE (2020c) Fabrication of gelatin/hydroxyapatite/3D-graphene scaffolds by a hydrogel 3D-printing method. Mater Chem Phys 239:122305. https://doi.org/10.1016/j.matchemphys.2019.122305
Nosrati H, Le DQS, Zolfaghari Emameh R, Canillas Perez M, Bünger CE (2021) Nucleation and growth of brushite crystals on the graphene sheets applicable in bone cement. Bol Soc Esp Ceram Vidrio. https://doi.org/10.1016/j.bsecv.2020.05.001
Okada T (1993) Complexation of poly(oxyethylene) in analytical chemistry a review. Analyst 118(8):959–971. https://doi.org/10.1039/AN9931800959
Oliveira JM, Rodrigues MT, Silva SS, Malafaya PB, Gomes ME, Viegas CA, Dias IR, Azevedo JT, Mano JF, Reis RL (2006) Novel hydroxyapatite/chitosan bilayered scaffold for osteochondral tissue-engineering applications: Scaffold design and its performance when seeded with goat bone marrow stromal cells. Biomaterials 27(36):6123–6137. https://doi.org/10.1016/j.biomaterials.2006.07.034
Pandey UB, Nichols CD (2011) Human disease models in drosophila melanogaster and the role of the fly in therapeutic drug discovery. Pharmacol Rev 63(2):411–436. https://doi.org/10.1124/pr.110.003293
Pappus SA, Ekka B, Sahu S, Sabat D, Dash P, Mishra M (2017) A toxicity assessment of hydroxyapatite nanoparticles on development and behaviour of *Drosophila melanogaster*. J Nanoparticle Res. https://doi.org/10.1007/s11051-017-3824-8
Photos PJ, Bacakova L, Discher Ba, Bates FS, Discher DE (2003) Polymer vesicles in vivo: correlations with PEG molecular weight. J Control Release 90:323–334
Posgai R, Ahamed M, Hussain SM, Rowe JJ, Nielsen MG (2009) Inhalation method for delivery of nanoparticles to the *Drosophila* respiratory system for toxicity testing. Sci Tot Environ 408(2):439–443. https://doi.org/10.1016/j.scitotenv.2009.10.008
Pramanik N, Bhargava P, Alam S, Pramanik P (2006) Processing and properties of nano- and macro-hydroxyapatite/poly(ethylene-co-acrylic acid) composites. Polym Compos 27(6):633–641. https://doi.org/10.1002/PC.20246
Pramanik S, Ataollahi F, Pingguan-Murphy B, Oshkour AA, Osman NAA (2015) In vitro study of surface modified poly(ethylene glycol)-impregnated sintered bovine bone scaffolds on human fibroblast cells. Sci Rep 5:1–11. https://doi.org/10.1038/srep09806
Ragaseema VM, Unnikrishnan S, Kalliyana Krishnan V, Krishnan LK (2012) The antithrombotic and antimicrobial properties of PEG-protected silver nanoparticle coated surfaces. Biomaterials 33(11):3083–3092. https://doi.org/10.1016/j.biomaterials.2012.01.005
Sapre N, Chakraborty R, Purohit P, Bhat S, Das G, Bajpe SR (2020) Enteric pH responsive cargo release from PDA and PEG coated mesoporous silica nanoparticles: a comparative study in *Drosophila melanogaster*. RSC Adv 10(20):11716–11726. https://doi.org/10.1039/c9ra11019d
Sarkar A, Mahendran TS, Meenakshisundaram A, Christopher RV, Dan P, Sundararajan V, Jana N, Venkatasubbu D, Sheik Mohideen S (2021) Role of cerium oxide nanoparticles in improving oxidative stress and developmental delays in *Drosophila melanogaster* as an in-vivo model for bisphenol a toxicity. Chemosphere 284:131363. https://doi.org/10.1016/j.chemosphere.2021.131363
Shrestha A, Hamblin MR, Kishen A (2012) Characterization of a conjugate between Rose Bengal and chitosan for targeted antibiofilm and tissue stabilization effects as a potential treatment of infected dentin. Antimicrob Agents Chemother 56(9):4876–4884. https://doi.org/10.1128/AAC.00810-12
Siepmann J, Podual K, Sriwongjanya M, Peppas NA, Bodmeirer (1999) A new model describing the swelling and drug release kinetics from hydroxypropyl methylcellulose tablets. J Pharm Sci 88(1):65–72. https://doi.org/10.1021/JS9802291
Siepmann F, Muschert S, Flament MP, Leterme P, Gayot J, Siepmann (2006) Controlled drug release from gelucire-based matrix pellets: experiment and theory. Int J Pharm 317(2):136–143. https://doi.org/10.1016/J.IJPHARM.2006.03.006
Su TT (2019) Drug screening in *Drosophila*; why, when, and when not? Wires Dev Biol 8(6):e346. https://doi.org/10.1002/wdev.346
Sundararajan V, Dan P, Kumar A, Venkatasubbu GD, Ichihara S, Ichihara G, Sheik Mohideen S (2019) Drosophila melanogaster as an in vivo model to study the potential toxicity of cerium oxide nanoparticles. Appl Surf Sci 490:70–80. https://doi.org/10.1016/j.apsusc.2019.06.017
Sundararajan V, Venkatsubbu GD, Sheik MS (2021) Investigation of therapeutic potential of cerium oxide nanoparticles in Alzheimer's disease using transgenic *Drosophila*. 3 Biotech 11:159. https://doi.org/10.1007/s13205-021-02706-x

Teixeira S, Rodriguez MA, Pena P, De Aza AH, De Aza S, Ferraz MP, Monteiro FJ (2009) Physical characterization of hydroxyapatite porous scaffolds for tissue engineering. Mater Sci Eng C 29:1510–1514. https://doi.org/10.1016/j.msec.2008.09.052

Tzafriri AR (2000) Mathematical modeling of diffusion-mediated release from bulk degrading matrices. J Controll 63(1–2):69–79. https://doi.org/10.1016/S0168-3659(99)00174-1

Venkatasubbu GD, Ramasamy S, Avadhani GS, Ramakrishnan V, Kumar J (2013) Surface modification and paclitaxel drug delivery of folic acid modified polyethylene glycol functionalized hydroxyapatite nanoparticles. Powder Technol 235:437–442. https://doi.org/10.1016/j.powtec.2012.11.003

Zeng X, Liu G, Tao W, Ma Y, Zhang X, He F, Pan J, Mei L, Pan G (2017) A drug-self-gated mesoporous antitumor nanoplatform based on ph-sensitive dynamic covalent bond. Adv Func Mater 27(11):1605985. https://doi.org/10.1002/ADFM.201605985

Zhu YJ (2017) Nanostructured materials of calcium phosphates and calcium silicates: synthesis, properties and applications. Chin J Chem 35(6):769–790. https://doi.org/10.1002/cjoc.201600696